

Towards Real-time Time-of-Arrival Self-Calibration using Ultra-Wideband Anchors

Kenneth Batstone, Magnus Oskarsson, Kalle Åström

Centre for Mathematical Sciences

Lund University

Lund, Sweden

Email: {kenneth_john.batstone, magnus.oskarsson, kalle}@math.lth.se

Abstract—Indoor localisation is a currently a key issue, from robotics to the Internet of Things. With hardware advancements making Ultra-Wideband devices more accurate and low powered (potentially even passive), this unlocks the potential of having such devices in common place around factories and homes, enabling an alternative method of navigation. Therefore, anchor calibration indoors becomes a key problem in order to implement these devices efficiently and effectively.

In this paper, we study the possibility for sequentially gathering Ultra-Wideband Time-of-Arrival measurements and using previously studied robust solvers, merge solutions together in order to calculate anchor positions in 3D in real-time. Here it is assumed that there is no prior knowledge of the anchor positions. This is then validated using Ultra-Wideband Time-of-Arrival data gathered by a Bitcraze Crazyflie quadcopter in 2D motion, 3D motion and full flight.

I. INTRODUCTION

Indoor positioning and navigation is a well known problem. In the modern world, systems such as GPS are heavily relied on for the navigation and positioning of people, vehicles and robots to name a few. Unfortunately, in highly urban areas, such as New York, tall buildings interfere with the accuracy of positioning and this becomes worse once inside any building. Once inside a building it can, at times, be impossible to acquire signals from the GPS satellites. When this occurs navigation users must use an alternative system. There are currently many options to overcome this problem but they all come with their own flaws. A large focus has been using the signal strength of Wi-Fi networks to perform positioning since the infrastructure currently exists in most buildings but due to the nature of radio signals, they have a low accuracy and with distance, the errors increase exponentially, [1]. Other options include Bluetooth devices (that have a short range) and dead reckoning approaches (that decrease in accuracy over time due to perturbations in errors).

Now, a new era of wireless communications, **5G** is hoping to bridge the gap to enable reliable indoor positioning. One such technology which is commercially available is Ultra-Wideband. The devices which use Ultra-Wideband are low powered and perform 2-way timing in order to obtain high precision in positioning, [2], between 2 devices. With further hardware advancements, Ultra-Wideband devices aim to be more accurate and lower powered (potentially even passive,

[3]). This unlocks the potential of having such devices in common place around factories and homes, enabling an alternative method of navigation indoors for people and Internet-of-Things (IoT) devices.

In this paper we present new research on methods for time-of-arrival (TOA) self-calibration problem. Here we exploit the factorisation of the receiver-transmitter distance matrix in order to enable real-time anchor calibration. This method is then applied to measurements taken using a Bitcraze, Crazyflie quadcopter with Ultra-Wideband anchors in order to determine if the proposed method is feasible in a real world situation, shown in Figure 1. These devices use the Decawave DWM1000 chip. For our experiments, the Ultra-Wideband anchors have the notation as either receiver or anchor, and the Crazyflie quadcopter as the transmitter.



Fig. 1. Image of the Ultra-Wideband anchor and Bitcraze Crazyflie quadcopter respectively from left to right.

The TOA self-calibration problem, is the problem of determining the positions of a number of receivers and transmitters given only receiver-transmitter distances. Here, there is no prior knowledge of the anchor positions. Hence, it is closely related to the anchor-free sensor network localisation problem [4] but differs, since our problem corresponds to a bipartite graph network, where [4] the network structure is a general graph. In [5], the authors explore the problem of embedded minimal rigid graphs in a larger general graph in order to solve the larger graph in the presence of missing information, which

is applicable to the TOA problem. The TOA problem also has certain similarities with the problem of determining a set of points given all inter-point distances, which is usually solved using multi-dimensional scaling [6].

Anchor-free sensor network calibration with time-of-arrival measurements has been investigated in a number of studies. Graph rigidity was explored in [4] to find a fold-free graph embedding, and the solution was then refined using mass-spring based optimisation. In [7], a semi-definite programming formulation and solution was proposed for TOA measurements, with or without anchors. Both of these methods are general for any solvable network structure, [8]. In an other line of work, there has been focused on sensor networks with a bipartite structure. For this type of network structure, one also aims to calculate the minimal problem, i.e. minimal number of receivers and transmitters required for the problem to be solvable. Note that for this problem, the roles of receivers and transmitters are equivalent. The minimal cases were studied in [9], which found that the minimal case of a 2D network is three transmitters and three receivers. The minimal problems for the 3D case are given in [10]. Here the minimal configuration of receivers and transmitters are (4, 6), (5, 5) and (6, 4) respectively. There are in general 38, 42 and 38 solutions respectively for the three types of problems. However, no practical methods for general 3D positions are given. There are a few results on algorithms for actually determining the positions from distances, most notably [11], [12]. In [13], a non-minimal linear solution to the 3D TOA self-calibration problem is derived for 10 (4) receivers and 4 (10) transmitters. In [14], [15] a solution is given to the TOA self-calibration problem, if one may additionally assume that one of the receivers coincides with the position of one of the transmitters.

Studying these minimal cases is of theoretical importance and further more essential when developing fast and stable algorithms based on robust estimation methods like RANSAC [16], in the presence of outliers in the measurements. As will be shown in the following sections, one important part of our system exploits that the so-called *compaction matrix* should have a certain rank. Low rank matrix factorisation has a long standing history. Truncating the singular value decomposition of the measurement matrix has been shown to give the optimal solution under the l^2 -norm for complete data, see [17]. The work in [18] was the first to consider missing data. Robustness to outliers has been considered in [19], [20], [21], [22]. Most methods mentioned above are based on alternating optimisation and are prone to get trapped in local minima. Recently, several works [23], [24], [25] re-formulate the problem to minimise the convex surrogate of the rank function, that is, the nuclear norm. For applications with a given fixed rank, the nuclear norm based methods usually perform inferior to the bilinear formulation-based methods [26]. A few recent works [27], [28], [29], [30] explore the idea of dividing the whole matrix into overlapping sub-blocks and combine the sub-block solutions. Minimal cases for low rank matrix factorisation, for missing data, were investigated

in [31]. This paper is a continuation of our paper [32], where a RANSAC paradigm was used in conjunction with minimal solvers and explored in order to obtain a robust and fast solution of the TOA self-calibration problem.

The novel concept of this paper, is that we can use our robust method to find a solution for a short dataset, then merge this solution sequentially to a previous solution. By doing this we see a convergent nature of calibrating the anchor positions in 2D and 3D as more data is collected. This has many added advantages. One such advantage is that it can be determined when there has been enough data acquired to solve the self calibration problem. In doing so, after the problem has been solved the user could switch to computationally lighter positioning algorithms to increase the performance. It also has the advantage of being implemented on large scales. As long as the solutions are connected, the solutions from one part of a building would be in the same coordinate system as another part of the building, but only the information from one part of the building is required to form a positioning solution, hence reducing the complexities of data storage and optimisations. In addition, since we are dealing with short datasets, these are quickly optimised to their local minima, so we have found overall improvements to our anchor positions calculations.

II. BASIC GEOMETRY

We will now describe the basic underlying geometry of our problem. Let \mathbf{r}_i , $i = 1, \dots, m$ and \mathbf{s}_j , $j = 1, \dots, n$ be the spatial coordinates of m receivers (e.g. Ultra-Wideband anchors) and n transmitters (e.g. Crazyflie quadcopter), respectively. For measured time of arrival t_{ij} from transmitter \mathbf{r}_i and receiver \mathbf{s}_j , we have $vt_{ij} = \|\mathbf{r}_i - \mathbf{s}_j\|_2$ where v is the speed of measured signals and $\|\cdot\|_2$ is the l^2 -norm. The speed v is assumed to be known and constant. We further assume that we, at each receiver can distinguish which transmitter j each event is originating from. This can be done e.g. if the signals are temporally separated or using different frequencies. We will in the following work with the distance measurements $d_{ij} = vt_{ij}$. It is quite common that such data contains both missing data from poor signal communications and outliers due to inaccuracies of the hardware measurements. The TOA calibration problem can then be defined as follows,

Problem 1: (Time-of-Arrival Self-Calibration) Given absolute distance measurements

$$d_{ij} = \|\mathbf{r}_i - \mathbf{s}_j\|_2 + \epsilon_{i,j}, \quad (1)$$

where the receiver positions are defined as \mathbf{r}_i , $i = 1, \dots, m$ and transmitter positions as \mathbf{s}_j , $j = 1, \dots, n$. Here the errors $\epsilon_{i,j}$ are assumed to be either **inliers**, in which case the errors are small ($\epsilon_{i,j} \in N(0, \sigma)$) or **outliers**, in which case the measurements are way off.

Here we will use the set W_i for the indices (i, j) corresponding to the inlier measurements.

We will now show how the TOA calibration problem is solved generally. From many types of media, a transmitter-

receiver distance will be acquired, d_{ij} . Since this can be assumed to be real and positive, it can be squared as follows,

$$d_{ij}^2 = (\mathbf{r}_i - \mathbf{s}_j)^T(\mathbf{r}_i - \mathbf{s}_j) = \mathbf{r}_i^T \mathbf{r}_i + \mathbf{s}_j^T \mathbf{s}_j - 2\mathbf{r}_i^T \mathbf{s}_j. \quad (2)$$

The problem is then reformed according to the following invertible linear combinations of d_{ij}^2 :

$$\mathbf{B} = \begin{pmatrix} d_{11}^2 & d_{12}^2 - d_{11}^2 & \dots & d_{1n}^2 - d_{11}^2 \\ d_{21}^2 - d_{11}^2 & \hat{\mathbf{B}} & & \\ \dots & & & \\ d_{m2}^2 - d_{11}^2 & & & \end{pmatrix}, \quad (3)$$

where the *compaction matrix* $\hat{\mathbf{B}}$ is an $(m-1) \times (n-1)$ matrix with entries as $\hat{B}_{ij} = \frac{d_{ij}^2 - d_{11}^2 - d_{1j}^2 + d_{11}^2}{-2}$, with $i = 2, \dots, m$ and $j = 2, \dots, n$. The other elements in \mathbf{B} are used as constraints for the solution.

The factorisation can then be interpreted as follows. Let $\mathbf{R}_i = [(\mathbf{r}_i - \mathbf{r}_1)]$ and $\mathbf{S}_j = [(\mathbf{s}_j - \mathbf{s}_1)]$. Here $\hat{\mathbf{B}} = \mathbf{R}^T \mathbf{S}$ with \mathbf{R}_i as columns of \mathbf{R} and \mathbf{S}_j as columns of \mathbf{S} . Since we assume that \mathbf{R} and \mathbf{S} are in a 3D affine space, the matrix $\hat{\mathbf{B}}$ has rank 3 at most. This also implies that in order to solve the problem, it is required that $m \geq 4$ and $n \geq 4$. By factorising $\hat{\mathbf{B}}$, we can compute the vectors to all receivers and transmitters from unknown initial/reference positions (\mathbf{r}_1 and \mathbf{s}_1).

By fixing \mathbf{r}_1 at the origin and \mathbf{s}_1 as a vector from the origin, in terms of an affine transformation matrix \mathbf{L} and vector \mathbf{b} , the problem is reformulated as follows,

$$\begin{aligned} \mathbf{r}_1 &= \mathbf{0}, \quad \mathbf{s}_1 = \mathbf{L}\mathbf{b}, \\ \mathbf{r}_i &= \mathbf{L}^{-T} \tilde{\mathbf{R}}_i, \quad i = 2 \dots m, \\ \mathbf{s}_j &= \mathbf{L}(\tilde{\mathbf{S}}_j + \mathbf{b}), \quad j = 2 \dots n, \end{aligned} \quad (4)$$

where $\tilde{\mathbf{R}} = \mathbf{L}^T \mathbf{R}$, $\tilde{\mathbf{S}} = \mathbf{L}^{-1} \mathbf{S}$, and hence $\hat{\mathbf{B}} = \tilde{\mathbf{R}}^T \mathbf{L}^{-1} \mathbf{L} \tilde{\mathbf{S}} = \mathbf{R}^T \mathbf{S}$.

Using this parametrisation, the equations from matrix \mathbf{B} , (3) become

$$\begin{aligned} d_{11}^2 &= (\mathbf{r}_1 - \mathbf{s}_1)^T(\mathbf{r}_1 - \mathbf{s}_1) = \mathbf{s}_1^T \mathbf{s}_1 = \mathbf{b}^T \mathbf{L}^T \mathbf{L} \mathbf{b} \\ &= \mathbf{b}^T \mathbf{H}^{-1} \mathbf{b}, \end{aligned} \quad (5)$$

$$\begin{aligned} d_{1j}^2 - d_{11}^2 &= \mathbf{s}_j^T \mathbf{s}_j - \mathbf{s}_1^T \mathbf{s}_1 = \tilde{\mathbf{S}}_j^T \mathbf{L}^T \mathbf{L} \tilde{\mathbf{S}}_j + 2\mathbf{b}^T \mathbf{L}^T \mathbf{L} \tilde{\mathbf{S}}_j \\ &= \tilde{\mathbf{S}}_j^T \mathbf{H}^{-1} \tilde{\mathbf{S}}_j + 2\mathbf{b}^T \mathbf{H}^{-1} \tilde{\mathbf{S}}_j, \end{aligned} \quad (6)$$

$$\begin{aligned} d_{i1}^2 - d_{11}^2 &= \mathbf{r}_i^T \mathbf{r}_i - 2\mathbf{r}_i^T \mathbf{s}_1 = \tilde{\mathbf{R}}_i^T (\mathbf{L}^T \mathbf{L})^{-1} \tilde{\mathbf{R}}_i - 2\mathbf{b}^T \tilde{\mathbf{R}}_i \\ &= \tilde{\mathbf{R}}_i^T \mathbf{H} \tilde{\mathbf{R}}_i - 2\mathbf{b}^T \tilde{\mathbf{R}}_i, \end{aligned} \quad (7)$$

where the symmetric matrix $\mathbf{H} = (\mathbf{L}^T \mathbf{L})^{-1}$. With this parametrisation, there are in total 9 unknowns (6 and 3 unknowns for \mathbf{H} and \mathbf{b} , respectively), and hence a solution can be found. Since this solution has its own coordinate system, with prior knowledge such as gyroscope data, this can be transformed back to the original coordinate system.

III. NON-LINEAR OPTIMISATION APPROACHES

In the development of the different systems for robust estimation, we use several local optimisation techniques. In particular we use methods for local optimisation of the type

$$\min_{\mathbf{r}, \mathbf{s}} \sum_{(i,j) \in \tilde{W}} f(d_{i,j} - \|\mathbf{r}_i - \mathbf{s}_j\|_2), \quad (8)$$

where $f(r)$ is chosen to be (i) $f(r) = r^2$ (l^2 -norm), (ii) $f(r) = |r|$ (l^1 -norm) or (iii) $f(r) = \min(r^2, T)$ (truncated l^2 -norm). If the subset \tilde{W} of the measurements contains no outliers and if the starting point is good, then the l^2 -norm can give good estimates. Optimising using the l^1 -norm is less sensitive to the subset \tilde{W} containing outliers, but still requires a reasonably good starting point to converge to a good solution. Local optimisation of the truncated l^2 -norm is even more sensitive to having a good starting point. Nevertheless, these local optimisation techniques are important components for designing robust systems.

IV. OBTAINING INITIAL ESTIMATES

Finding the optimal solution to problem 1, in the presence of outliers and missing data is a highly non-convex problem. We are thus dependent on finding good initial starting solutions, for the optimisation methods from the previous section to work. We will in this section describe the different initialisation methods that we have used in our experiment. In the next section we will describe our latest contribution to the initialisation problem.

Arguably, the most straight-forward way to initialise a solution, is to simply randomly place all receivers and transmitters within some space. This usually gives poor initial estimates, and the local optimisation will be prone to get stuck in local minima. A slight improvement to this idea, is to use multiple restarts and optimise from each initial position, and then in the end choose the best solution.

Another way of initialising, that we have explored, is using the rank constraint on the compaction matrix. Here one can use many existing methods for doing the low rank matrix factorisation. One important draw-back of these methods, is that we need to have at least one row and one column of the data matrix completely known, and without outliers. The last criteria is of course hard to check. If all data is known, the optimal low rank factorisation is given by singular value decomposition (SVD) of the data matrix. A heuristic for handling missing data, is simply to fill in the missing data with some random values that follow the statistics of the other known measurements. One can then use SVD to obtain an initial estimate. This can be used directly to find the solution to the original problem as described in section II. Alternatively, the initial low rank matrix factorisation can be refined using the Wiberg algorithm, [18].

V. RANDOM SAMPLING PARADIGM

The RANSAC or hypothesis and test paradigm, has proven to be useful in situations where there are outliers in the data, [16]. In this paradigm, a subset of the data is used to estimate

the unknown parameters. The remainder of the data is then used to verify or falsify the parameters. This is typically repeated a fixed number of iterations. The parameters that give the largest number of inliers are then usually used as an initial estimate for the subsequent non-linear optimisation of the parameters.

For Problem 1, there are several ways one could implement the hypothesis and test paradigm.

One idea would be to use efficient algorithms for determining receiver and transmitters positions from minimal data, [10]. Although this solver and the test is relatively fast, we propose an alternative to this approach. In one of our recent papers the idea is to find a fast way to hypothesise and test. We will use the rank constraints of the compaction matrix to do this. Our method is described in [32].

VI. MERGING SOLUTIONS

Assume that there are two sequential solutions $\hat{\mathbf{B}}_1 = \mathbf{R}_1^T \mathbf{S}_1$ and $\hat{\mathbf{B}}_2 = \mathbf{R}_2^T \mathbf{S}_2$. Within these two solutions there exists a subset of data that overlaps denoted by a subscript, i . Since the two solutions are in different coordinate systems, due to coordinate dis-ambiguities in our solutions, then the idea is to find a transformation matrix $Q \in \mathbb{R}^{K \times K}$ to transform \mathbf{R}_2 into the same coordinate system as \mathbf{R}_1 . Using this transformation matrix, the solution can be transformed to another coordinated system where the solution is just as valid, i.e.

$$\mathbf{R}_2^T \mathbf{S}_2 = \mathbf{R}_2^T Q Q^{-1} \mathbf{S}_2. \quad (9)$$

Since there is an overlapping region, i , in the solutions, it can be assumed that

$$\mathbf{R}_{1,i}^T \mathbf{S}_{1,i} = (\mathbf{R}_{2,i}^T Q) (Q^{-1} \mathbf{S}_{2,i}), \quad (10)$$

and hence,

$$\mathbf{R}_{1,i}^T = \mathbf{R}_{2,i}^T Q, \quad (11)$$

$$\mathbf{S}_{2,i} = Q \mathbf{S}_{1,i}. \quad (12)$$

Provided there is enough data in the overlapping region (11) and (12), then the transformation matrix Q can be solved linearly. The two solutions can then be merged, the overlapping region $\mathbf{R}_{1,i}, \mathbf{S}_{1,i}$ is updated using (11), (12) and the rest of $\mathbf{R}_2, \mathbf{S}_2$ are concatenated onto the previous solution using (9). Since \mathbf{R} and \mathbf{S} are linear combinations of \mathbf{r} and \mathbf{s} , then the compaction matrix doesn't need to be calculated in order to solve this, instead \mathbf{r} and \mathbf{s} are used to calculate Q . The details of our algorithm are explained in Algorithm 1.

Algorithm 1 Our Solution merging scheme

- 1: Select Overlapping region such that it is assumed that $\mathbf{r}_1 = \mathbf{r}_2$
 - 2: Calculate the transformation matrix in a RANSAC way to obtain the best Q .
 - 3: **If:** when applying the best transformation matrix Q , the new solution does not fit well i.e. $\|\mathbf{r}_{1,i}^T - \mathbf{r}_{2,i}^T Q\|_2 + \|\mathbf{s}_{1,i}^T - Q \mathbf{s}_{2,i}^T\|_2 > \epsilon$, for some sufficiently small ϵ , then \mathbf{r}_1 remains the same and \mathbf{s}_2 are trilaterated points using \mathbf{r}_1 .
 - 4: **Else:** Calculate the new $\mathbf{r}_{1,i}$ and \mathbf{s}_2 according to (11) and (12).
 - 5: Optimise over the range of both solutions.
-

VII. EXPERIMENTAL SETUP

To test our method 3 experiments were conducted using a Bitcraze Crazyflie quadcopter and their Loco-positioning system which consists of Ultra-Wideband chips on the anchors and quadcopter. Six anchors were positioned around the rooms and for two of the experiments, measured using a laser distance meter to obtain ground truth positions of the anchors in the 2D experiment and full flight experiment with an error of $\pm 2 \text{ mm}$.

The other experiment was conducted in a MOCAP studio to record the ground truth flightpath as well as the anchor positions with an error of $\pm 1 \text{ mm}$.

Distance measurements from the quadcopter to all the anchors were measured at a frequency of 30 Hz .

Two of the experimental environments were rooms in an office block, which reduced the chances of large outliers or missing data, but the 2D experiment was performed in a large open space in an office block with meeting rooms in the centre in order to provoke large amounts of missing data.

The experiments were conducted by moving the quadcopter, by hand, around the room except for the full flight experiment, where the quadcopter was flown. The distance measurements were recorded so that they may be processed offline. Our algorithms do not require any prior knowledge of anchor or quadcopter positions. The only requirement is that our minimal solver (5,5) is satisfied for the 3D cases and (3,3) for the 2D case.

VIII. EXPERIMENTAL EVALUATION

Once the measurements were taken, they were streamed into our algorithm to simulate real-time acquisition. At all optimisation steps, l^2 optimisation on the inlier set was performed. We also added a smoothness prior in the optimisation. This prior is based on minimising acceleration, according to

$$res_a = \frac{1}{\sigma_a^2} \sum_{j=2}^{n-1} \|\mathbf{s}_{j-1} - 2\mathbf{s}_j + \mathbf{s}_{j+1}\|_2^2, \quad (13)$$

where σ_a is a parameter controlling the strength of the smoothness prior. This is reasonable since the motion of the quadcopter is continuous.

A. MOCAP Experiment

When streaming the data, a number of buffer lengths were tested, in order to see if this had an effect on the rate of convergence. The result of this can be seen in Figure 2. To show this result a Procrustes fitting was used to find a transformation between the ground truth anchor positions and the final calculated anchor positions. This transform was then applied to all calculated solutions retrospectively so that they are in equivalent coordinate systems. In the Procrustes fitting only rotation and translation were allowed.

A buffer length of 20 measurements was then chosen for the subsequent experiments.

Using the same set-up and data from the MOCAP studio, solutions were found for each 20 measurement and merged together using 10 overlapping measurements. As before a

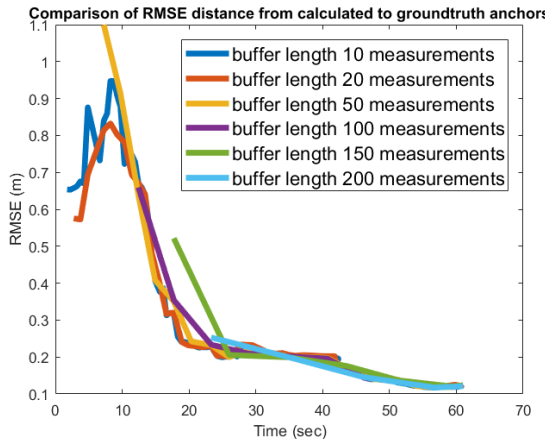


Fig. 2. This figure illustrates the Root Mean Squared Error (RMSE) distance between the calculated to ground truth anchor positions for different buffered measurement sizes.

retrospective Procrustes fitting was applied. Here the (5,5) minimal solver was used.

To show the convergence of each of the anchor positions, the distance from the calculated anchor position to the ground truth anchor positions are plotted for each step, as shown in Figure 3.

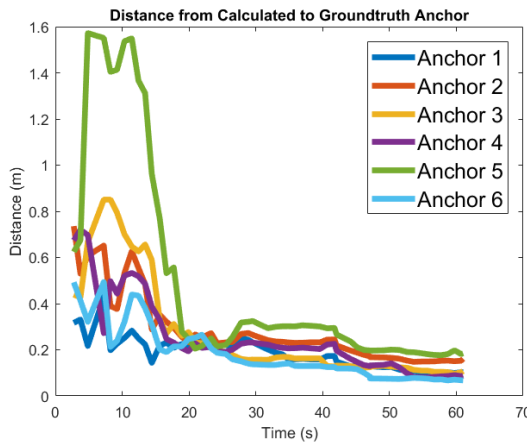


Fig. 3. This figure illustrates the distance between the calculated to ground truth anchor positions.

Here the final distance from the calculated anchor position to the ground truth anchor positions are as follows, $(0.1026, 0.1612, 0.1078, 0.0888, 0.1845, 0.0675)m$ for anchors 1 to 6 respectively.

The final solution is shown in Figure 4. In this figure, three instances from sequentially calculating and merging solutions are shown with the last being the final solution. In this dataset there was 0.61% of the data missing. For the final solution, the distance from each quadcopter positions to the corresponding ground truth position was calculated. A histogram of the errors can be seen in Figure 5.

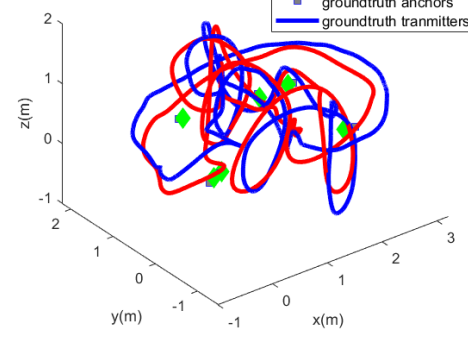
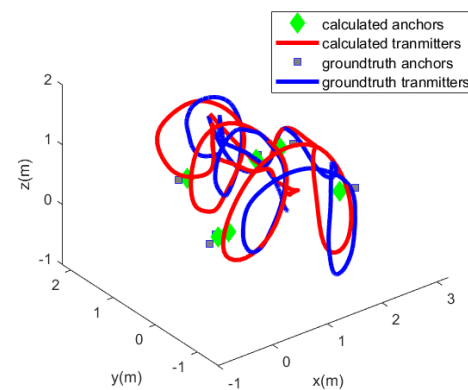
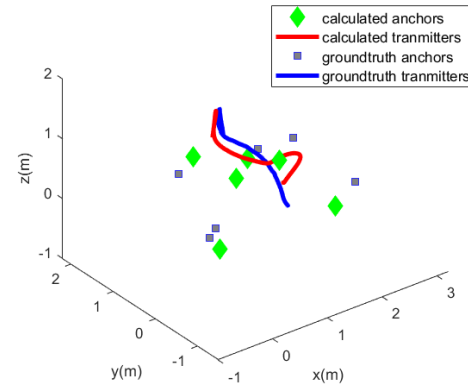


Fig. 4. The figure illustrates the estimated anchor positions and quadcopter positions. These are overlaid on the ground truth anchor positions and flightpath. Each graph represents a different, (increasing) time instance, the bottom corresponding to the final solution.

B. Full Flight Experiment

During this experiment, a video recording of the experiment was made. In Figure 6, three of the video frames are shown with the 3D-points projected onto the image. The main purpose is to be able to visualise the convergence of the anchor positions during a flight. Here the (5,5) minimal solver was used.

Here the distance from the final calculated anchor po-

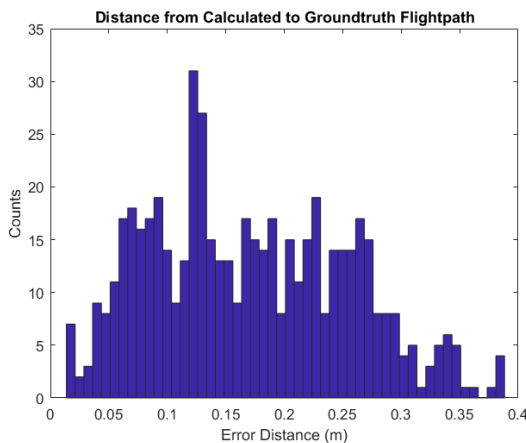


Fig. 5. This figure illustrates the distance between the calculated to ground truth anchor positions.

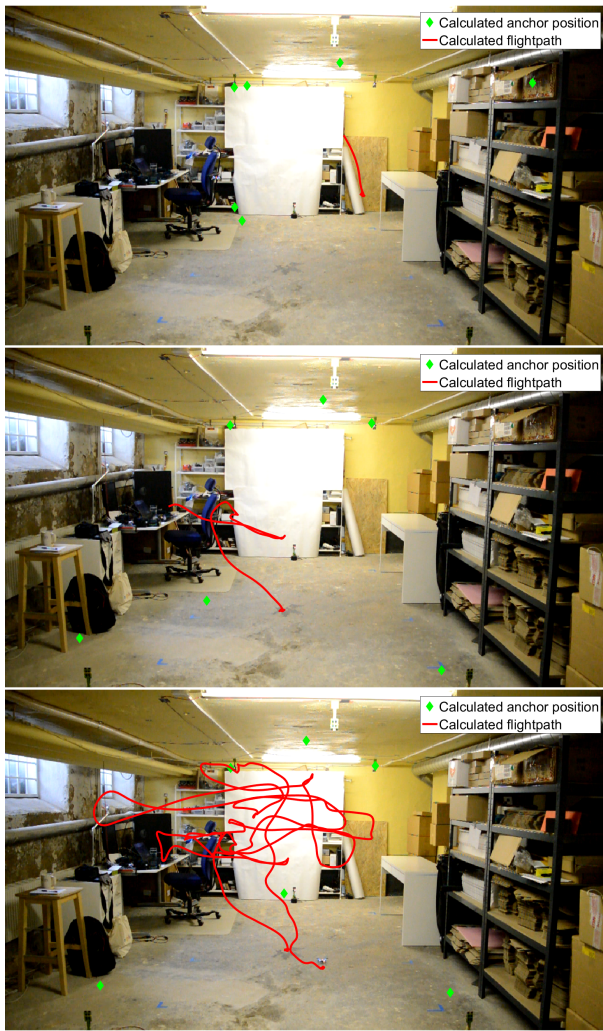


Fig. 6. These figures illustrate the estimated anchor positions and the flightpath positions at various times of the flight to show how the anchor positions are updated. The positions of the quadcopter and the anchors can be seen in the photographs.

sition to the ground truth anchor positions are as follows, $(0.1439, 0.1154, 0.1501, 0.1664, 0.1477, 0.1842)m$, for anchors 1 to 6 respectively. In this dataset there was 0.01% of the data missing. Again, a retrospective Procrustes fitting was applied as before.

C. 2D Experiment

The main purpose of this experiment is to be able to visualise the convergence of the anchor positions and to be able to test the robustness of our algorithm. Due to the short range of the UWB devices and the obstacle of the Meeting Rooms, there was no instance of a given quadcopter position having full distance measurements to all 6 anchors. In this dataset there was 49.61% of the data missing. Here the (3,3) minimal solver was used.

Here the distance from the final calculated anchor position to the ground truth anchor positions are as follows, $(0.0814, 0.1717, 0.0702, 0.1392, 0.1700, 0.2017)m$, for anchors 1 to 6 respectively. Again a retrospective Procrustes fitting was applied as before.

IX. CONCLUSIONS

In this paper, a novel method has been constructed to take advantage of the factorisation of the transmitter-receiver matrix in order to push for real-time Ultra-Wideband anchor calibration. This has been verified using TOA Ultra-Wideband measurement data in a streamed way to simulate real-time calculations.

Looking at Figure 2, it can be seen that regardless of the buffer length, each solution converges to a similar solution. Once the system acquires a sufficient amount of data, they all converge. This then implies, by having a shorter buffer length then there would be more instances to test to see if a final solution has been met and therefore be able to move over to a computationally lighter positioning algorithm. It is also worth noting, that the there was a slight improvement in the final solution when the buffer length was smaller. Here the buffer length of 10 measurements gave the best solution. This may be due to higher frequency of optimisation steps, which would allow the calculated solutions to be closer to the global optimum, hence the solution to the next iteration would have a better initialisation, which is important in this highly non-linear system. Although a smaller buffer length tends to improve the final result, caution must be taken. The smaller the buffer length, the less robust our solver becomes so the errors from one section could affect the subsequent solutions and the final solution. This effect was seen on occasions, but UWB in line-of-sight situations produces accurate measurements so it didn't often occur and the buffer length was increased to 20 measurement to ensure robustness.

Looking at the results from the MOCAP studio experiments, Figures 3, 4 & 5, it can be seen that this method produces accurate results. For current Ultra-Wideband systems, the chip sets come with a recommended accuracy of $\pm 0.2m$. From our results we are also able to achieve this accuracy, as seen from the convergent plots Figure 2 & 3. Further to this,

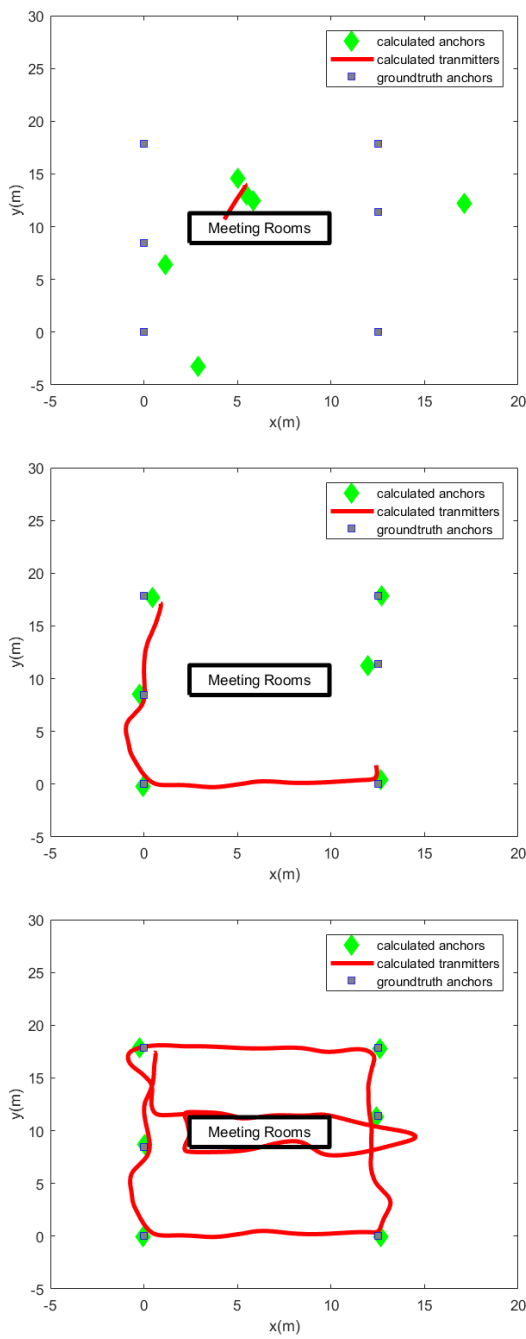


Fig. 7. This figure illustrates the estimated anchor positions and the quadcopter positions. This is overlaid on the ground truth anchor positions. The central rectangle represents the Meeting rooms which provoked missing data. Each graph represents a different (increasing) time instance, the last being the final solution.

each time we process the data, we reach a similar result. This would lead us to believe that we have achieved the global optima. It is also interesting to note that the convergence of the anchor positions to their true positions is not monotonic. It shows potentially at points in time that not enough data has been collected to make a reasonable solution but once it does have enough data, the convergence is rapid and the previous

solutions are then corrected. This is further demonstrated in Figure 6.

In the 2D experiment, our algorithms were pushed in order to test the robustness of the system in the presence of large amounts of missing data. From Figure 7 it can be seen that the anchor positions are calculated to a high accuracy despite 49.61% of missing data. At most given quadcopter positions, it could acquire at most 4 distance measurements to the anchors. The minimum required number of overlapping anchors for the merging scheme to function is 2, any less and the 2 solution sets would be disjointed so it would be impossible to merge the coordinate systems. This data set, however, does show that our real-time scheme could be implemented on a large scale. As long as the criterion for the merging scheme is met then the system can be extended substantially. Only the local anchors to the quadcopter are needed for self-calibration of the anchors and relative positioning of the quadcopter. The previous solutions are only needed to have a common coordinate system. This then implies that if enough data is collected in a single area, then when the quadcopter moves to another area, only the anchor positions need to be stored and the data from that area would not be needed in further optimisation steps. This would allow for much faster computations and hybrid self-calibration/trilateration algorithms.

For future work, the study of this convergent nature would be interesting in order to produce a viable method for a stopping condition for calibrating the anchor positions. By solving this problem it would allow for large scale navigation and positioning with no need for prior knowledge of the anchor positions, it would also be less computationally intensive which is preferable for robots and IoT devices.

ACKNOWLEDGEMENTS

The authors would like to thank the people at Bitcraze AB for all their support. The author would also like to thank MAPCI, ELLIIT and Royal Physiographic Society of Lund for funding.

REFERENCES

- [1] B. Li, J. Salter, A. G. Dempster, and C. Rizos, "Indoor positioning techniques based on wireless lan," in *LAN, FIRST IEEE INTERNATIONAL CONFERENCE ON WIRELESS BROADBAND AND ULTRA WIDEBAND COMMUNICATIONS*, pp. 13–16.
- [2] A. A. Adebowehin and S. D. Walker, "Enhanced ultrawideband methods for 5g los sufficient positioning and mitigation," in *2016 IEEE 17th International Symposium on A World of Wireless, Mobile and Multimedia Networks (WoWMoM)*, June 2016, pp. 1–4.
- [3] F. Dowla, F. Nekoogar, D. Benzel, G. Dallum, and A. Spiridon, "Method of remote powering and detecting multiple uwb passive tags in an rfid system," May 29 2012, uS Patent 8,188,841. [Online]. Available: <https://www.google.ch/patents/US8188841>
- [4] N. Priyantha, H. Balakrishnan, E. Demaine, and S. Teller, "Anchor-free distributed localization in sensor networks," in *Proceedings of the 1st international conference on Embedded networked sensor systems*. ACM, 2003, pp. 340–341.
- [5] M. Oskarsson, K. Åström, and A. Torstensson, *Prime Rigid Graphs and Multidimensional Scaling with Missing Data*. IEEE-Institute of Electrical and Electronics Engineers Inc., 2014, pp. 750–755.
- [6] G. Young and A. Householder, "Discussion of a set of points in terms of their mutual distances," *Psychometrika*, vol. 3, no. 1, pp. 19–22, 1938.
- [7] P. Biswas, T.-C. Lian, T.-C. Wang, and Y. Ye, "Semidefinite programming based algorithms for sensor network localization," *ACM Trans. Sen. Netw.*, vol. 2, no. 2, pp. 188–220, May 2006. [Online]. Available: <http://doi.acm.org/10.1145/1149283.1149286>
- [8] T. Eren, O. Goldenberg, W. Whiteley, Y. Yang, A. Morse, B. Anderson, and P. Belhumeur, "Rigidity, computation, and randomization in network localization," in *INFOCOM 2004. Twenty-third Annual Joint Conference of the IEEE Computer and Communications Societies*, vol. 4. IEEE, 2004, pp. 2673–2684.
- [9] H. Stewénius, "Gröbner basis methods for minimal problems in computer vision," Ph.D. dissertation, Lund University, APR 2005.
- [10] Y. Kuang, S. Burgess, A. Torstensson, and K. Åström, "A complete characterization and solution to the microphone position self-calibration problem," in *The 38th International Conference on Acoustics, Speech, and Signal Processing*, 2013.
- [11] S. Burgess, Y. Kuang, and K. Åström, "Node localization in unsynchronized time of arrival sensor networks," in *Proceedings of the 21st International Conference on Pattern Recognition*, 2012.
- [12] ———, "Pose estimation from minimal dual-receiver configurations," in *Proceedings of the 21st International Conference on Pattern Recognition*, 2012.
- [13] M. Pollefeys and D. Nister, "Direct computation of sound and microphone locations from time-difference-of-arrival data," in *Proc. of International Conference on Acoustics, Speech and Signal Processing*, 2008.
- [14] M. Crocco, A. Del Bue, M. Bustreo, and V. Murino, "A closed form solution to the microphone position self-calibration problem," in *37th International Conference on Acoustics, Speech, and Signal Processing (ICASSP 2012), Kyoto, Japan*, March 2012.
- [15] M. Crocco, A. Del Bue, and V. Murino, "A bilinear approach to the position self-calibration of multiple sensors," *Trans. Sig. Proc.*, vol. 60, no. 2, pp. 660–673, feb 2012. [Online]. Available: <http://dx.doi.org/10.1109/TSP.2011.2175387>
- [16] M. A. Fischler and R. C. Bolles, "Random sample consensus: a paradigm for model fitting with applications to image analysis and automated cartography," *Communications of the ACM*, vol. 24, no. 6, pp. 381–95, 1981.
- [17] C. Eckart and G. Young, "The approximation of one matrix by another of lower rank," *Psychometrika*, vol. 1, no. 3, pp. 211–218, 1936. [Online]. Available: <http://dx.doi.org/10.1007/BF02288367>
- [18] T. Wiberg, "Computation of principal components when data are missing," in *Proc. Second Symp. Computational Statistics*, 1976.
- [19] H. Aanaes, R. Fisker, K. Åström, and J. Carstensen, "Robust factorization," *IEEE Trans. Pattern Analysis and Machine Intelligence*, 2002.
- [20] A. M. Buchanan and A. W. Fitzgibbon, "Damped newton algorithms for matrix factorization with missing data," in *Proceedings of the 2005 IEEE Computer Society Conference on Computer Vision and Pattern Recognition (CVPR'05) - Volume 2 - Volume 02*, ser. CVPR '05. Washington, DC, USA: IEEE Computer Society, 2005, pp. 316–322. [Online]. Available: <http://dx.doi.org/10.1109/CVPR.2005.118>
- [21] Q. Ke and T. Kanade, "Robust L_1 norm factorization in the presence of outliers and missing data by alternative convex programming," in *Proc. Conf. Computer Vision and Pattern Recognition*, 2005.
- [22] A. Eriksson and A. Hengel, "Efficient computation of robust weighted low-rank matrix approximations using the L_1 norm," *IEEE Trans. Pattern Analysis and Machine Intelligence*, 2012.
- [23] E. J. Candès, X. Li, Y. Ma, and J. Wright, "Robust principal component analysis?" *Journal of ACM*, 2009.
- [24] R. Garg, A. Roussos, and L. Agapito, "Dense variational reconstruction of non-rigid surfaces from monocular video," in *Computer Vision and Pattern Recognition (CVPR), 2013 IEEE Conference on*. IEEE, 2013, pp. 1272–1279.
- [25] C. Olsson and M. Oskarsson, "A convex approach to low rank matrix approximation with missing data," in *Scandinavian Conf. on Image Analysis*, 2011.
- [26] R. Cabral, F. D. la Torre, J. P. Costeira, and A. Bernardino, "Unifying nuclear norm and bilinear factorization approaches for low-rank matrix decomposition," in *Proc. Int. Conf. on Computer Vision*, 2013.
- [27] L. W. Mackey, M. I. Jordan, and A. Talwalkar, "Divide-and-conquer matrix factorization," in *Advances in Neural Information Processing Systems*, 2011, pp. 1134–1142.
- [28] V. Larsson, C. Olsson, E. Bylow, and F. Kahl, "Rank minimization with structured data patterns," in *ECCV*, 2014.
- [29] C. Julià, A. D. Sappa, F. Lumbreras, J. Serrat, and A. López, "An iterative multiresolution scheme for sfm with missing data," *Journal of Mathematical Imaging and Vision*, vol. 34, no. 3, pp. 240–258, 2009.
- [30] V. Larsson and C. Olsson, "Convex envelopes for low rank approximation," in *EMMCVPR 2015*, 2015.
- [31] F. Jiang, M. Oskarsson, and K. Åström, "On the minimal problems of low-rank matrix factorization," in *Proc. Conf. Computer Vision and Pattern Recognition*, 2015.
- [32] K. Batstone, M. Oskarsson, and K. Åström, "Robust time-of-arrival self calibration and indoor localization using wi-fi round-trip time measurements," in *2016 IEEE International Conference on Communications Workshops (ICC)*, May 2016, pp. 26–31.